Published in final edited form as:
Mol Cancer Res. 2011 November ; 9(11): 1449–1461. doi:10.1158/1541-7786.MCR-11-0100.

ADAM12 produced by tumor cells rather than stromal cells accelerates breast tumor progression

Camilla Fröhlich[1], **Camilla Nehammer**[1], **Reidar Albrechtsen**[1], **Pauliina Kronqvist**[2], **Marie Kveiborg**[1], **Atsuko Sehara-Fujisawa**[3], **Arthur M. Mercurio**[4], and **Ulla M. Wewer**[1,*]

[1]Department of Biomedical Sciences and Biotech Research & Innovation Centre (BRIC), University of Copenhagen, Ole Maaløes Vej 5, 2200 Copenhagen N, Denmark [2]Department of Pathology, University of Turku, 20520 Turku, Finland [3]Department of Growth Regulation, Institute for Frontier Medical Sciences, Kyoto University, Kyoto 606-8507, Japan [4]Department of Cancer Biology, University of Massachusetts Medical School, Worcester, MA 01605, USA

Abstract

Expression of ADAM12 is low in most normal tissues, but is markedly increased in numerous human cancers, including breast carcinomas. We have previously shown that overexpression of ADAM12 accelerates tumor progression in a mouse model of breast cancer (PyMT). In the present study, we found that ADAM12 deficiency reduces breast tumor progression in the PyMT model. However, the catalytic activity of ADAM12 appears to be dispensable for its tumor-promoting effect. Interestingly, we demonstrate that ADAM12 endogenously expressed in tumor-associated stroma in the PyMT model does not influence tumor progression, but that ADAM12 expression by tumor cells is necessary for tumor progression in these mice. This finding is consistent with our observation that in human breast carcinoma ADAM12 is almost exclusively located in tumor cells and only rarely seen in the tumor-associated stroma. We hypothesized, however, that the tumor-associated stroma may stimulate ADAM12 expression in tumor cells, based on the fact that TGF-β1 stimulates ADAM12 expression and is a well-known growth factor released from tumor-associated stroma. TGF-β1 stimulation of ADAM12-negative Lewis lung tumor cells induced ADAM12 synthesis, and growth of these cells *in vivo* induced a >200-fold increase in ADAM12 expression. Our observation that ADAM12 expression is significantly higher in the terminal duct lobular units (TDLUs) adjacent to human breast carcinoma compared with TDLUs found in normal breast tissue supports our hypothesis that tumor-associated stroma triggers ADAM12 expression.

Keywords

ADAM12; breast cancer; TGF-β1; stroma; tumor cells

Introduction

Breast cancer continues to be one of the leading causes of death among women in Western countries. Each year, close to 200,000 women are diagnosed with breast cancer in the United States, and, despite improved screening for early detection as well as improved treatment modalities, approximately 40,000 U.S. women die of the disease (1).

*Corresponding author. Contact information: Ulla M. Wewer, Department of Biomedical Sciences and Biotech Research & Innovation Centre (BRIC), University of Copenhagen, Ole Maaløes Vej 5, 2200 Copenhagen N, Denmark, ullaw@sund.ku.dk.

The authors declare that they have no conflicts of interest.

Tumors are composed not only of neoplastic cells, but also of stromal cells including myofibroblasts, angiogenic and inflammatory cells that reside in the extracellular matrix. Cell-cell and cell-matrix interactions between tumor cells, the surrounding stromal cells, and the extracellular matrix ignite cascades of molecular signals in and out of cells, modulating cell behavior and contributing to tumor progression (2-4). Metalloproteases are among the key proteins associated with malignancy (4, 5). One such metalloprotease, ADAM12 (Meltrin alpha), has recently been found to be a candidate breast cancer susceptibility gene (6). ADAM12 is a member of the large ADAM family of transmembrane proteins and has several potentially important biological functions in cancer (reviewed in (7, 8)). At the molecular level, ADAM12 can -as many other ADAMs (8, 9)-mediate proteolytic ectodomain shedding of growth factors and cell adhesion molecules (7, 8, 10). Importantly, ADAM12 is also involved in nonproteolytic protein-protein interactions–e.g., it binds to integrins, syndecans, and transforming growth factor (TGF) β receptor II (TGFβRII) at the cell surface, and its intracellular tail associates with adaptors and signalling molecules (such as Grb2, Tks5, and Src kinases) (7, 8).

In normal tissue, expression of ADAM12 is generally low; however, several studies have reported that the expression of ADAM12 is markedly increased in many human cancers, including breast (11-15), liver (16), bladder (17), and lung (18, 19) carcinomas and glioblastomas (20), and that the level of expression often relates to tumor stage. The potential use of ADAM12 as a biomarker for tumor progression was further evidenced by the finding that soluble ADAM12 in urine from breast and bladder cancer patients correlates with disease stage (17, 21, 22). We have previously demonstrated that overexpression of ADAM12 promotes tumor progression in the mouse mammary tumor virus (MMTV)-polyoma middle T antigen (PyMT) model (12). This discovery correlates with the finding that ADAM12 deficiency reduces tumor progression in the TRAMP mouse model of prostate cancer (23).

Here, we explored how endogenous ADAM12 impacts breast tumor progression. In particular, we investigated the role of ADAM12 localization in the stromal compartment versus the tumor compartment in promoting tumor progression. To answer this question, we established an *in vivo* model system to investigate whether ADAM12 produced by the stromal cells in mouse mammary-gland tumors influences tumor progression. The data demonstrate that ADAM12 produced by tumor cells promotes tumor progression whereas ADAM12 expressed by the tumor-associated stroma did not. Interestingly, however, we observed that TGF-β1, known to be produced by the tumor-associated stroma, influences expression of ADAM12 in the tumor cell compartment. In addition, we observed that the proteolytic activity of ADAM12 appears to be dispensable for this tumor-promoting effect.

Thus, we hypothesize that the effect of ADAM12 -that is, increased proliferation and dedifferentiation could be mediated through enhanced TGF-β1 signalling provided by the surrounding stroma.

Materials and Methods

Mice

Male FVB/N-TgN(MMTV-PyMT)634Mul (Jackson Laboratory, Bar Harbor, ME) mice were mated with ADAM12 (Meltrin alpha)-deficient (ADAM12 -/-) female mice (24) that had been previously backcrossed for 9 generations into the FVB/N background. Male PyMT-ADAM12+/- offspring were mated with female ADAM12-/- mice to obtain PyMT-ADAM12-/- and littermate PyMT-ADAM12+/- mice. All animals analyzed in this study were females and examined as previously described (12). Wild-type, ADAM12+/-, and ADAM12-/- mice on C57/Bl6 and FVB/N genetic backgrounds were used for injections of

tumor cells. Cell lines (10^6 cells per mouse) were injected subcutaneously into the right flank or into the mammary gland. Tumor size (length and width) was measured over time. Mice were sacrificed when the first tumor reached 1.2 cm^2. One hour before sacrifice, 5-bromo-2′-deoxyuridine (BrdU; 50 μg/g body weight) was injected intraperitoneally (i.p.), subsequently mice were anesthetized by i.p. administration of a 1:1 mixture of Dormicum and Hypnorm. Tumors were removed and the mice were perfusion fixed with cold PBS followed by cold 4% paraformaldehyde. Lungs were removed, fixed and cryoembedded as described (25). Tumor burden was calculated as the percentage of tumor mass/mouse weight. Tumor volume was estimated according to the formula; $V(\text{tumor}) = \pi l w^2/6$ (26). All experiments were conducted in accordance with the guidelines of the Animal Experiment Inspectorate, Denmark.

Cell culture

Lewis Lung carcinoma cells (American Type Culture Collection, Rockville, MD) and B16F10 melanoma cells (generously provided by Finsen Laboratory, Denmark) were grown in Dulbecco's Modified Eagle Medium (DMEM), 1% GlutaMAX (Invitrogen, Tårstrup, Denmark), 50 units/mL penicillin, 50 μg/mL streptomycin, and 10% fetal bovine serum (FBS) at 37°C and 5% CO_2. Cells were incubated for 24 hours with serum-free DMEM with or without TGF-β1 (Sigma-Aldrich, Brøndby, Denmark) as indicated.

To generate primary tumor cells, tumors from 8–10-week-old PyMT-ADAM12-/- mice and their littermate controls were harvested, minced into small pieces, and tumor cells isolated as described (27). Freshly isolated cells were plated on collagen type I (PureCol from Advanced Biomatrix, San Diego, CA) and grown for 24 hours in DMEM, penicillin/streptomycin, and 10% FBS. Vital and adherent cells were harvested and immediately frozen or used for immortalization.

To generate immortalized PyMT cell lines, pBABE-PyMT (Addgene, Cambridge, MA (plasmid 22305)) (27) was retrovirally transduced as described previously (28) into primary tumor cells isolated from PyMT-ADAM12+/- and PyMT-ADAM12-/- mice. Cells were kept in DMEM with 50 μg/mL hygromycin B. The established cell line deficient in ADAM12 expression was termed PyMT-A12null, whereas the control cell line expressing ADAM12 was termed PyMT-A12hz (hz for heterozygous). PyMT-A12null cells stably expressing human ADAM12-L lacking the cytoplasmic tail (hADAM12Δcyt), hADAM12Acyt with a catalytic site mutation (hADAM12Δcyt-E351Q), or vector control were generated by retroviral transduction as described (12). The ADAM12-E351Q mutant was previously shown to be proteolytic inactive (29-31). The cytoplasmic tail of ADAM12 retains ectopically expressed ADAM12 in the *trans*-Golgi network; hence, to ensure accurate ADAM12 expression at the plasma membrane, hADAM12Δcyt was used (32). The established cell lines were designated PyMT-A12, PyMT-A12EQ, and PyMT-VC, respectively, and kept in DMEM containing 4 μg/mL puromycin and 50 μg/mL hygromycin B.

Staining and analysis of mouse tissue and cells

Mammary-gland tumors were obtained from PyMT-ADAM12-/- mice and PyMT-ADAM12+/- littermates and processed for histological analysis as described (12, 33, 34). Briefly, the histological evaluation was based on a four-stage classification scheme that includes hyperplasia, adenoma, and early and late carcinoma (34). These stages are in agreement with the recommendations for classifications of mouse mammary tumor pathology (33), but improved for the PyMT model (34). Areas of early and late carcinoma as well as hyperplasia and adenoma areas were marked and the areas estimated by two independent observers as described (12, 34). To evaluate cell proliferation, DNA synthesis

was determined using BrdU *in vivo* labelling and subsequent detection with an anti-BrdU antibody (Roche, Hvidovre, Denmark). Immunohistochemical staining of mouse tissue was performed with the rb109 antibody against ADAM12 or affinity purified ADAM12 polyclonal antibody from ProteinTech Group (Chicago, IL) as described (28).

Cell proliferation in cultured cells was determined using the Clik-it EdU Imaging kit (Invitrogen) that allows incorporation of the thymidine analog 5-ethynyl-2′-deoxyuridine (EdU) into DNA during active DNA synthesis. Briefly, PyMT-A12hz, PyMT-A12null, PyMT-A12, PyMT-A12EQ, and PyMT-VC cells were seeded on collagen coated dishes and allowed to recover for 16 hours. The cells were treated with 10μM EdU and incubated for 30min at 37°C to enable EdU-incorporation. Subsequently, the cells were fixed, permeabilized and stained with Alexa Flour® azide and cell nuclei were detected with DAPI. The fraction of cells with incorporated EdU was detected by flourescence microscopy and analysed by MetaMorph software.

Cells plated on collagen-coated 35-mm dishes were fixed (4% paraformaldehyde), permeabilized (0.1% Triton X-100), incubated with anti-mouse pan-cytokeratin antibody (Dako, Glostrup, Denmark) (1:200) or normal mouse IgG (10μg/ml) followed by incubation with Alexa 488-conjugated anti mouse IgG antibody (Invitrogen), and then stained with 4′, 6-diamidino-2-phenylindole (DAPI; Invitrogen). Cells were mounted using fluorescent mounting medium (Dako), and fluorescence imaging was performed using an inverted Zeiss Axiovert 220 Apotome system equipped with a 63x/1.4 Plan-Apochromat water immersion objective. The images were processed using the Axiovision program (Carl Zeiss, Jena, Germany).

Reverse transcription-PCR (RT-PCR) and quantitative PCR (qPCR)

Total RNA was extracted and isolated from mouse tissue and mouse cell lines using Trizol (Invitrogen). RNA (1 μg) was treated with DNase I and reverse-transcribed using the High-Capacity cDNA RT-kit from Applied Biosystems (Carlsbad, CA). RT-PCR was conducted using TEMPase Hot Start DNA and Polymerase (Ampliqon, Skovlunde, Denmark). The RT-PCR program used was: 15 minutes at 95°C followed by 35 cycles of 15 seconds at 96°C, 20 seconds at 55°C, and 60 seconds at 72°C, and finally 5 minutes at 72°C. qPCR was performed using SYBR Green PCR Mastermix from Applied Biosystems. The qPCR program used was: 2 minutes at 50°C and 10 minutes at 95°C, followed by 40 cycles of 15 seconds at 95°C, 60 seconds at 60°C. Primers used for both RT-PCR and qPCR were for the reference gene rPO (forward, 5′-TTCATTGTGGGAGCAGAC-3′; reverse, 5′-CAGCAGTTTCTCCAGAGC-3′), glyceraldehyde 3-phosphate dehydrogenase (GADPH): (forward, 5′ -AAGGTCATCCCAGAGCTGAACG-3′; reverse, 5′-TGTCATACCAGGAAATGAGC-3′), and ADAM12 (forward, 5′-TGTGGAAATGGCTATGTGGA-3′; reverse, 5′-CAGGTGGTAGCGTTACAGCA-3′). qPCR data were analyzed using the 2(-ΔΔC(t)) method (35).

Western blot

Western blots of cell lysates were performed as described previously (36). For immunoprecipitation cells were lysed in RIPA buffer with inhibitors (Complete® EDTA-free, Pierce and Halt™ Phosphatase Inhibitor Cocktail, Thermo Scientific), 800 μg of total cell protein lysate were incubated with 2 μg of EGFR antibody (Upstate, NY), rotated for 16 hours at 4 °C, and subsequently 50 μl of protein-A-Sepharose (Amersham Biosciences) was added. Following incubation with rotation for 2 h at 4 °C, the immune complex was washed with RIPA buffer and eluted in SDS sample buffer prior subjected to electrophoresis and blotting. To enrich for glycoproteins, cell lysates were subjected to concanavalin A agarose beads (Sigma-Aldrich) and eluted as described (37) prior to electrophoresis and blotting.

Following protein separation by SDS-PAGE and transfer to Immobilon-P membranes (Millipore Corp., Billerica, MA), indicated antibodies were added and incubated 16 hours at 4 °C. Horseradish peroxidase (HRP)-conjugated anti-rabbit IgG and anti-mouse IgG antibodies (Dako, Glostrup, Denmark) and the chemiluminescence EZ-ECL reagent (Biological Industries, Fredensborg, Denmark) were used for detection. Primary antibodies used for detections were: ADAM12 (polyclonal rabbit rb122 (12)), p-Akt (ser473) and Akt (Cell Signaling Technology, Danvers, MA), EGFR (Upstate), pTyr (Santa Cruz Biotechnology Inc, CA), E-cadherin (Santa Cruz Biotechnology Inc), actin (Millipore A/S, Copenhagen, Denmark).

Human breast carcinoma specimens

Six breast cancer tissue arrays representing 805 women diagnosed with breast cancer during the years 1988–2005 were analyzed (Table 1A). In addition, specimens from breast resections of 61 patients who underwent conservation surgery for a breast lump at Turku University Hospital (Turku, Finland) were analyzed. To prepare macrosections, fresh surgical breast tissue was sliced at 5-mm intervals through the specimen. Each tissue slice was visualized with mammography to ensure excision of the whole tumor area. All tissue slices were then separately and in sequence fixed in formalin, embedded in paraffin in 5 × 5 cm macroblocks, cut into 5-μm sections, and H&E stained. From these macroblocks, 1–3 representative areas were excised, re-embedded in paraffin, and 5-μm sections cut for staining. From the same hospital, normal breast tissue was obtained from 10 patients who underwent aesthetic breast-reduction surgery. The experimental use of the surgical specimens was in accordance with the hospital ethical guidelines of Turku University Hospital.

ADAM12 immunohistochemistry of human breast tissue

ADAM12 immunostaining was performed as described earlier (11, 12), using either polyclonal antibodies to human ADAM12 (rb109, rb116, or rb122; 1:250 dilution) or normal rabbit IgG fraction (10 μg/mL) prepared in PBS. Detection was performed using the DakoChemMate detection kit (Dako). Examination of the 805 cases was performed as an overall evaluation of positive or negative ADAM12 immunostaining. Examination of the 61 macroblocks was performed in more detail. The intensity and distribution of ADAM12 staining in benign and malignant breast epithelial cells were evaluated independently by two pathologists. Staining of the surrounding stroma for ADAM12 was evaluated in all cases, and evaluation of breast terminal duct lobular units (TDLUs) further than 5 mm away from the carcinoma cells was performed.

Statistical analysis

Statistical analysis was done using Kaplan-Meier to determine tumor-free periods, and the log-rank test, the Wilcoxon Signed-Rank test, and the Student's *t* test for comparing two independent groups. $P < 0.05$ was considered statistically significant.

Results and Discussion

ADAM12 deficiency delays PyMT-induced mammary tumorigenesis

To elucidate the role of ADAM12 in breast cancer, we analyzed the effect of ADAM12 deficiency on mammary-tumor growth in the PyMT mouse model of breast cancer. ADAM12-deficient mice were cross-bred with MMTV-PyMT mice and analyzed for tumor onset and progression. PyMT-ADAM12-/- mice developed palpable breast tumors at a significantly slower rate than did PyMT-ADAM12+/- mice (Fig. 1A). In the PyMT-ADAM12-/- cohort, tumors in female offspring appeared at day 73±12 (mean ±SD),

whereas PyMT-ADAM12+/- mice developed tumors by day 61±8. The tumor burden was significantly decreased in PyMT-ADAM12-/- mice at 12 weeks of age, as compared with age-matched PyMT-ADAM12+/- mice (Fig. 1B). Histopathological examination of H&E-stained sections of breast tissue was performed to analyze tumor grade (degree of differentiation), as described (12, 34). We evaluated the percentage of early and late carcinoma as well as hyperplasia and adenoma areas within the mammary-gland tumors (34) and found a significant reduction of areas of early and late carcinoma in the tumors from PyMT-ADAM12-/- mice as compared with PyMT-ADAM12+/- mice (Fig. 1 C and D). In addition to developing spontaneous breast tumors, PyMT mice have a high incidence of lung metastasis. Thus, the percentage of mice bearing at least one tumor nodule was determined by histological examinations as exemplified in Figure 1E. The incidence of lung metastasis was 55% in PyMT-ADAM12hz mice (6/11) and 9% in PyMT-ADAM12null mice (1/11) (Fig. 1F). Taken together, these data demonstrate that ADAM12 significantly influences tumor initiation and progression, confirming and extending previous reports (12, 15, 23).

ADAM12 affects the proliferative capacity of PyMT tumor cells

Based on previous studies proposing that ADAM12 may influence tumor cell proliferation (13, 20, 38, 39), we hypothesized that endogenous ADAM12 in the PyMT mouse model regulates cancer cell proliferation. Therefore, BrdU incorporation was assessed in PyMT-ADAM12-/- and PyMT-ADAM12+/- tumors. A significant decrease in tumor cell proliferation was observed in the PyMT-ADAM12-/- tumors compared with PyMT-ADAM12+/- tumors (Fig. 2A). To study the observed difference in tumor cell proliferation in more detail, tumor cells from both PyMT-ADAM12-/- and PyMT-ADAM12+/- mice were isolated, immortalized, and grown *in vitro*. Immunofluorescence staining using an antibody against cytokeratins confirmed that the immortalized PyMT-A12null and PyMT-A12hz cell lines were of epithelial origin (Supplemental Fig. 1A). RT-PCR and Western blotting confirmed the endogenous expression of ADAM12 in PyMT-A12hz tumor cells and a lack of ADAM12 expression in the PyMT-A12null tumor cells (Fig. 2B and C). Next, the proliferative capacity of the two tumor cell lines was compared by *in vitro* and *in vivo* assays. The PyMT-A12null tumor cells showed a significantly reduced proliferative capacity *in vitro* compared with PyMT-A12hz tumor cells (Fig. 2D). Accordingly, when the PyMT-A12null and PyMT-A12hz cells were injected into the mammary gland of wild-type or ADAM12-/- mice, the PyMT-A12null cells grew significantly slower than the PyMT-A12hz tumor cells (Fig. 2E and F). Although there is a significant difference between proliferation of PyMT-A12hz and PyMT-A12null tumor cells *in vitro*, we reason that the more pronounced difference in *in vivo* tumor cell growth relates to the tumor-stroma interactions. Similarly, PyMT-A12hz cells injected subcutaneously gave rise to significantly larger tumors compared to PyMT-A12null cells (Supplemental Fig. 1B). Intriguing, we observed that orthotopic injection of the tumor cells gave rise to larger tumors when compared to subcutaneously injected tumor cell (Fig. 2E,F and Supplemental Fig. 1B). A potential explanation could be that the microenvironment and thereby growth conditions in the mammary fat pad of mice are different and more advantageous for breast tumor cells than when these cells are injected subcutaneously in the dorsal flank as previously suggested (40). Taken together, these results support the notion that the PyMT-A12null tumor cells had a reduced growth capacity compared with ADAM12-expressing PyMT-A12hz tumor cells. Importantly, the findings also suggest that ADAM12 specifically produced by the tumor cells confers accelerated tumor progression in the PyMT mouse model.

To begin to unravel the molecular mechanism behind the decreased tumor cell proliferation in the absence of ADAM12, we tested the hypothesis that ADAM12 stimulates Akt signaling, a known inducer of cell proliferation. Interestingly, levels of phosphorylated Akt were decreased by approximately 50% in PyMT-A12null compared to PyMT-A12hz tumor

cells (Fig. 2G), suggesting that ADAM12 expression in PyMT tumor cells stimulates growth via the Akt signalling pathway.

The proteolytic activity of ADAM12 is dispensable for ADAM12-accelerated PyMT tumor progression

The proteolytic activity of ADAM12 has been shown to involve ectodomain shedding and the consequent release of epidermal growth factor (EGF) receptor (EGFR) ligands (20, 24, 29, 31, 39, 41, 42). Ligand binding of EGFR contributes to the activation of numerous intracellular signalling pathways, such as proliferation and differentiation, which are important for tumor progression (43). Instantly, the key question remaining to be answered is whether the proteolytic activity of ADAM12 is required for its tumor-promoting effect in the PyMT model. Hence, we expressed human ADAM12, a proteolytically inactive mutant form of human ADAM12 (ADAM12EQ) (29-31) or the empty vector (as a control) into PyMT-A12null tumor cells. The resulting three new cell lines–PyMT-A12, PyMT-A12EQ, and PyMT-VC–were studied. Western blotting demonstrated that ADAM12 was expressed in both the PyMT-A12 and PyMT-A12EQ cells, but not in the PyMT-VC cells (Fig. 3A). The proliferative capacity of the three tumor cell lines was compared by *in vitro* and *in vivo* assays. Interestingly, both PyMT-A12 and PyMT-A12EQ tumor cells showed a significantly increased proliferative capacity *in vitro* compared with PyMT-VC tumor cells (Figure 3B). However, the proliferative index between PyMT-A12 and PyMT-A12EQ tumor cells was not significantly different. The three cell lines were subsequently injected into the mammary gland (Fig. 3C) or subcutaneously in the right flank (Fig. 3D) of ADAM12+/- mice. Similarly to the *in vitro* proliferation data, both PyMT-A12 and PyMT-A12EQ cells produced tumors of significantly increased final tumor volume as compared with the PyMT-VC cells. The growth pattern of tumors produced by PyMT-A12EQ and PyMT-A12 cells were not significantly different. In support of these data, overexpression of ADAM12 in PyMT cells did not induce phosphorylation of EGFR (Fig. 3E), suggesting that ADAM12 is not involved in ectodomain shedding and the consequent release of EGFR ligands, such as EGF and HB-EGF in these cell lines. However, we found that both PyMT-A12 and PyMT-A12EQ tumor cells exhibited higher levels of phosphorylated Akt compared to PyMT-VC tumor cells (Fig. 3F), indicating that ADAM12 independent of its proteolytic activity may stimulate Akt signaling to support tumor cell proliferation. Taken together, these results suggest that the effect of ADAM12 on tumor progression in the PyMT model system is not dependent on its proteolytic activity. Although these data contrast with the finding that ADAM12 positively correlates with the proliferative index in human glioblastomas and the ability to shed proheparin binding-EGF (20), they substantiate the reports that ADAM10 and ADAM17 are the main sheddases of EGFR ligands (44, 45).

Based on the observed findings, we hypothesize that the protumorigenic effect of ADAM12 may likely be mediated by its disintegrin and the cysteine-rich domains, which have important functions in protein-protein interactions (46-50)). The recombinant disintegrin domain of ADAM12 as well as full-length ADAM12-S has been previously shown to bind integrins (47-54) and impair the function of β1-integrin, consequently altering the organization of the actin cytoskeleton and extracellular matrix (28). Moreover, the extracellular domains of ADAM12 interact with TGFβRII and contribute to TGFβ signaling (46). Notably, Akt, which activation is increased in both PyMT-A12 and PyMT-A12EQ mutant cells as compared to control (Fig. 3F), is a downstream target in both integrin and TGFβRII signaling cascades known to affect proliferation and survival (55, 56). While it remains to be elucidated whether ADAM12 interacts with these molecules in breast tumor cells *in vivo*, it is intriguing that deletion of both β1-integrin and focal adhesion kinase, a major mediator of integrin signaling, suppresses PyMT-mediated tumor initiation and progression in animal models (27, 57).

Stromal ADAM12 does not influence tumor growth in PyMT-mediated breast tumors

ADAM12 mRNA is endogenously expressed in α-smooth muscle actin (α-SMA)-positive stromal cells in the PyMT breast cancer model and in the W^{10} prostate cancer model (23). In addition, ADAM12 expression in stroma is required for prostate tumor progression. However, our data (Fig. 2) indicate that ADAM12 produced by the tumor cells is essential for tumor progression in the PyMT model. These findings raise the question of what effect ADAM12 produced by the stromal cells has on the reduced breast-tumor growth in PyMT-ADAM12-/- mice. To answer this question, we first confirmed that stromal cells in normal mouse mammary gland express ADAM12 by immunohistochemistry (Fig. 4A). Next, to determine the role of ADAM12 produced by the stromal-cell compartment on PyMT tumor progression, PyMT-A12hz and PyMT-A12null cells were injected into the mammary gland (Fig. 4B and C) or subcutaneously (Fig. 4D and E) into ADAM12-/- mice (ADAM12-negative stroma) and their littermate controls (wild-type and ADAM12+/- mice; ADAM12-positive stroma). Interestingly, for both PyMT-A12null and PyMT-A12hz tumor cells there was no difference in growth whether the stroma contained ADAM12 (wild-type and ADAM12+/- mice) or not (ADAM12-/- mice). These results indicate that ADAM12 produced by the stromal compartment does not significantly influence tumor growth in the PyMT model.

To further test the putative role of ADAM12 produced by murine stromal cells, B16F10 melanoma cells were injected subcutaneously into wild-type, ADAM12+/-, and ADAM12 -/- mice. No difference was observed in the growth of tumors injected into the three different types of recipient mice (Supplemental Figure 2), indicating that ADAM12 expressed by the stromal compartment has no impact on the growth of the B16F10 melanoma cells. Collectively, these data reveal that stromal expression of ADAM12, as demonstrated by three different cell lines (PyMT-A12hz, PyMT-A12null, B16F10) in two different stromal compartments (subcutaneous space and the mammary gland), does not influence tumor growth. Although the stromal compartment is the major source of several matrix metalloproteinases with important roles in tumor progression and invasion (4, 58), our data strongly indicate that only tumor cell expression of ADAM12 contributes to tumor progression.

ADAM12 is produced by tumor cells in human breast cancer

The relevance of our findings to human breast carcinoma is significant. Previous studies of ADAM12 expression in breast carcinomas have reported that it is highly expressed in carcinoma cells but that it is not detected in the stroma (11, 12, 14, 17, 18). To verify this conclusion, we analyzed the ADAM12 distribution pattern by immunohistochemistry in human breast carcinoma specimens from 805 cases, arranged in 6 separate tissue arrays. A total of almost 63% of the cases exhibited positive ADAM12 immunoreactivity of the tumor cells (Table 1A), whereas stromal cells were generally not positive for ADAM12 immunostaining (data not shown). To further support these observations, we analyzed ADAM12 immunoreactivity in malignant breast lesions in sections obtained from 61 cases in which macroblocks had been prepared (Supplemental Fig. 3). Detailed semi-quantitative immunohistochemical analyses (Table 1B) demonstrated that ADAM12 immunoreactivity was found in 47% of IDC and 97% of ILC samples studied. Furthermore, areas containing ADH and/or DCIS in addition to tumor cells were selected (see insert in Supplemental Fig. 3A). We observed ADAM12 immunoreactivity in 77% of the epithelial cells in ADH and 84% of epithelial cells in DCIS. Of all the tissue specimens that exhibited positive ADAM12 immunoreactivity, only the breast epithelial cells were found to be positive for ADAM12 (Fig. 5A and B). In few cases, a few stromal cells exhibited positive staining for ADAM12 (data not shown). These data confirm previous observations that, in human breast cancer,

ADAM12 expression is almost exclusively located in tumor cells, and only rarely seen in the tumor-associated stroma (11-13).

Tumor-associated stroma induces ADAM12 expression in the epithelium

The expression of ADAM12 is low in most normal tissues, but relatively high in many human cancers. Given our observation that the tumor cells in breast cancers are responsible for the increased ADAM12 expression, we investigated potential factors that could trigger induction of ADAM12 in these tumor cells. Specifically, we hypothesized that tumor-associated stroma influences ADAM12 expression in tumor cells because it is known that interactions between cancer cells and stromal components influence tumor growth and progression (4). The tumor-associated stromal cells encompass a number of cells with a broadly similar phenotype, known as reactive fibroblasts, myofibroblasts, or carcinoma-associated fibroblasts (2, 3). These cells have received increased attention because of their contribution to tumor development and progression through the release of a number of cytokines. Among these cytokines, TGF-β1 (59) is frequently referred to as having strong effects on both tumor growth and invasion by increased proliferation, dedifferentiation, and enhanced EMT (4, 59, 60). Interestingly, TGF-β1 is a known transcriptional regulator of ADAM12 (16) and has been demonstrated to upregulate ADAM12 transcription in several cancer cell lines including the breast cancer cell line MDA-MB-231 (61). Hence, we analyzed whether tumor-stromal interactions or the tumor-associated stroma could regulate the expression of ADAM12 in cells normally not expressing the protein, potentially through TGF-β1 action. For this purpose, we took advantage of Lewis Lung cells, which express no or low levels of ADAM12 *in vitro* (Fig. 6A), and which are syngeneic with the ADAM12-deficient mouse strain. Initially, we demonstrated that stimulation of Lewis Lung cells with TGF-β1 *in vitro* increased the expression of ADAM12, as assessed by RT-PCR, qPCR, and Western Blot (Fig. 6B,C,D). Subsequently, Lewis Lung cells were injected subcutaneously into wild-type, ADAM12+/-, or ADAM12-/- mice and, as expected, no difference in tumor growth was seen (Fig. 6E). However, the ADAM12 transcript was >200-fold up-regulated in Lewis Lung tumors formed in ADAM12-/- mice compared with Lewis Lung cells grown *in vitro* (Fig. 6F), indicating that the stroma compartment or tumor-stroma interaction initiate tumor cell expression of ADAM12. In comparison, the level of ADAM12 mRNA in the Lewis Lung tumor tissue in wild-type and ADAM12+/- mice was much higher than in tumors from ADAM12-/- mice (Fig. 6G), suggesting that ADAM12 is expressed in the stroma compartment as also shown in Figure 4A. Immunohistochemistry staining of ADAM12 in Lewis Lung cells grown as subcutaneous tumors confirm the presence of ADAM12 protein in the tumor cells (Supplemental Fig. 4). These data support the hypothesis that tumor-associated stroma induces ADAM12 expression in tumor cells and they suggest the possibility that TGF-β1 may be one stromal factor that contributes to ADAM12 expression (46).

To analyze if changes in tumor-associated stroma have the ability to influence expression of ADAM12 in human breast tissue, we analyzed the macroblocks from human breast cancer patients described above. These macroblocks enabled us to perform immunohistochemical evaluation of ADAM12 expression in extended areas of the surrounding tissue from 45 cases of invasive carcinomas. In particular, we were able to examine the TDLUs adjacent to the carcinomas in greater detail (Supplemental Fig. 3). ADAM12 immunostaining was clearly increased both in distribution and intensity in the TDLUs adjacent to the invasive tumor compared with the normal TDLUs from breast reductions (Fig. 5C and D). Whereas 89% of epithelial cells in the TDLUs adjacent to invasive carcinomas were positive for ADAM12, only 28% in the normal TDLUs in breast-reduction tissue showed positive ADAM12 immunostaining (Table 1C). This result could imply that humoral factors (i.e., TGF-β1) from the malignant tumor or the tumor-associated stroma might influence

expression of ADAM12 in the breast epithelium in the TDLUs adjacent to the malignant tumor. Indeed, a recent study demonstrated that TGF-β1 is up-regulated at the interface between the periphery of breast tumor tissue and normal adjacent tissue compared with normal tissue (62).

Together, the data presented here strongly emphasize the importance of endogenous ADAM12 for efficient tumor development. Intriguingly, the pro-tumorigenic effect of ADAM12 appears to involve nonproteolytic mechanisms. Moreover, our data imply that the stroma may trigger ADAM12 expression in tumor cells and TDLUs adjacent to tumor cells, even though ADAM12 expression in the stroma is not important for tumor growth in the mouse models studied. Based on these findings, we propose that ADAM12 expression in tumor cells contributes to their proliferation and de-differentiation.

Supplementary Material

Refer to Web version on PubMed Central for supplementary material.

Acknowledgments

We thank Brit Estreich and Zulfiya Sukhova in our laboratory and Agnieszka Ingvorsenc from the Finsen Laboratory Rigshospitalet for technical assistance; and Linda Raab for editing the manuscript.

Grant support: Danish Cancer Society (DP08019), Munksholm, Dansk Kræftforsknings Fond and NIH Grant CA80789.

Reference List

1. Alterkruse, SF.; Kosary, CL.; Krapcho, M.; Neyman, N.; Aminou, R.; Waldron, W., et al. SEER Cancer Statistics Review, 1975-2007. National Cancer Institute; Bethesda: 2011. http://seer.cancer.gov/cse/1975_2007/
2. Arendt LM, Rudnick JA, Keller PJ, Kuperwasser C. Stroma in breast development and disease. Semin Cell Dev Biol. 2010; 21:11–8. [PubMed: 19857593]
3. Pietras K, Ostman A. Hallmarks of cancer: interactions with the tumor stroma. Exp Cell Res. 2010; 316:1324–31. [PubMed: 20211171]
4. Egeblad M, Nakasone ES, Werb Z. Tumors as organs: complex tissues that interface with the entire organism. Dev Cell. 2010; 18:884–901. [PubMed: 20627072]
5. Kruger A, Kates RE, Edwards DR. Avoiding spam in the proteolytic internet: future strategies for anti-metastatic MMP inhibition. Biochim Biophys Acta. 2010; 1803:95–102. [PubMed: 19800374]
6. Sjoblom T, Jones S, Wood LD, Parsons DW, Lin J, Barber TD, et al. The consensus coding sequences of human breast and colorectal cancers. Science. 2006; 314:268–74. [PubMed: 16959974]
7. Kveiborg M, Albrechtsen R, Couchman JR, Wewer UM. Cellular roles of ADAM12 in health and disease. Int J Biochem Cell Biol. 2008; 40:1685–702. [PubMed: 18342566]
8. Edwards DR, Handsley MM, Pennington CJ. The ADAM metalloproteinases. Mol Aspects Med. 2008; 29:258–89. [PubMed: 18762209]
9. Iida A, Sakaguchi K, Sato K, Sakurai H, Nishimura D, Iwaki A, et al. Metalloprotease-dependent onset of blood circulation in zebrafish. Curr Biol. 2010; 20:1110–6. [PubMed: 20605457]
10. Jacobsen J, Wewer UM. Targeting ADAM12 in human disease: head, body or tail? Curr Pharm Des. 2009; 15:2300–10. [PubMed: 19601832]
11. Iba K, Albrechtsen R, Gilpin BJ, Loechel F, Wewer UM. Cysteine-rich domain of human ADAM 12 (meltrin alpha) supports tumor cell adhesion. Am J Pathol. 1999; 154:1489–501. [PubMed: 10329602]
12. Kveiborg M, Frohlich C, Albrechtsen R, Tischler V, Dietrich N, Holck P, et al. A role for ADAM12 in breast tumor progression and stromal cell apoptosis. Cancer Res. 2005; 65:4754–61. [PubMed: 15930294]

13. Lendeckel U, Kohl J, Arndt M, Carl-McGrath S, Donat H, Rocken C. Increased expression of ADAM family members in human breast cancer and breast cancer cell lines. J Cancer Res Clin Oncol. 2005; 131:41–8. [PubMed: 15565459]

14. Narita D, Anghel A, Seclaman E, Ilina R, Cireap N, Ursoniu S. Molecular profiling of ADAM12 gene in breast cancers. Rom J Morphol Embryol. 2010; 51:669–76. [PubMed: 21103624]

15. Roy R, Rodig S, Bielenberg D, Zurakowski D, Moses MA. ADAM12 transmembrane and secreted isoforms promote breast tumor growth: A distinct role for ADAM12-S in tumor metastasis. J Biol Chem. 2011

16. Le PH, Bonnier D, Wewer UM, Coutand A, Musso O, Baffet G, et al. ADAM12 in human liver cancers: TGF-beta-regulated expression in stellate cells is associated with matrix remodeling. Hepatology. 2003; 37:1056–66. [PubMed: 12717386]

17. Frohlich C, Albrechtsen R, Dyrskjot L, Rudkjaer L, Orntoft TF, Wewer UM. Molecular profiling of ADAM12 in human bladder cancer. Clin Cancer Res. 2006; 12:7359–68. [PubMed: 17189408]

18. Mino N, Miyahara R, Nakayama E, Takahashi T, Takahashi A, Iwakiri S, et al. A disintegrin and metalloprotease 12 (ADAM12) is a prognostic factor in resected pathological stage I lung adenocarcinoma. J Surg Oncol. 2009; 100:267–72. [PubMed: 19544357]

19. Rocks N, Paulissen G, Quesada CF, Polette M, Gueders M, Munaut C, et al. Expression of a disintegrin and metalloprotease (ADAM and ADAMTS) enzymes in human non-small-cell lung carcinomas (NSCLC). Br J Cancer. 2006; 94:724–30. [PubMed: 16495931]

20. Kodama T, Ikeda E, Okada A, Ohtsuka T, Shimoda M, Shiomi T, et al. ADAM12 is selectively overexpressed in human glioblastomas and is associated with glioblastoma cell proliferation and shedding of heparin-binding epidermal growth factor. Am J Pathol. 2004; 165:1743–53. [PubMed: 15509542]

21. Pories SE, Zurakowski D, Roy R, Lamb CC, Raza S, Exarhopoulos A, et al. Urinary metalloproteinases: noninvasive biomarkers for breast cancer risk assessment. Cancer Epidemiol Biomarkers Prev. 2008; 17:1034–42. [PubMed: 18483323]

22. Roy R, Wewer UM, Zurakowski D, Pories SE, Moses MA. ADAM 12 cleaves extracellular matrix proteins and correlates with cancer status and stage. J Biol Chem. 2004; 279:51323–30. [PubMed: 15381692]

23. Peduto L, Reuter VE, Sehara-Fujisawa A, Shaffer DR, Scher HI, Blobel CP. ADAM12 is highly expressed in carcinoma-associated stroma and is required for mouse prostate tumor progression. Oncogene. 2006; 25:5462–6. [PubMed: 16607276]

24. Kurisaki T, Masuda A, Sudo K, Sakagami J, Higashiyama S, Matsuda Y, et al. Phenotypic analysis of Meltrin alpha (ADAM12)-deficient mice: involvement of Meltrin alpha in adipogenesis and myogenesis. Mol Cell Biol. 2003; 23:55–61. [PubMed: 12482960]

25. Nielsen BS, Lund LR, Christensen IJ, Johnsen M, Usher PA, Wulf-Andersen L, et al. A precise and efficient stereological method for determining murine lung metastasis volumes. Am J Pathol. 2001; 158:1997–2003. [PubMed: 11395377]

26. Euhus DM, Hudd C, LaRegina MC, Johnson FE. Tumor measurement in the nude mouse. J Surg Oncol. 1986; 31:229–34. [PubMed: 3724177]

27. Pylayeva Y, Gillen KM, Gerald W, Beggs HE, Reichardt LF, Giancotti FG. Ras- and PI3K-dependent breast tumorigenesis in mice and humans requires focal adhesion kinase signaling. J Clin Invest. 2009; 119:252–66. [PubMed: 19147981]

28. Kawaguchi N, Sundberg C, Kveiborg M, Moghadaszadeh B, Asmar M, Dietrich N, et al. ADAM12 induces actin cytoskeleton and extracellular matrix reorganization during early adipocyte differentiation by regulating beta1 integrin function. J Cell Sci. 2003; 116:3893–904. [PubMed: 12915587]

29. Albrechtsen R, Stautz D, Sanjay A, Kveiborg M, Wewer UM. Extracellular engagement of ADAM12 induces clusters of invadopodia with localized ectodomain shedding activity. Exp Cell Res. 2011; 317:195–209. [PubMed: 20951132]

30. Jacobsen J, Visse R, Sorensen HP, Enghild JJ, Brew K, Wewer UM, et al. Catalytic properties of ADAM12 and its domain deletion mutants. Biochemistry. 2008; 47:537–47. [PubMed: 18081311]

31. Kveiborg M, Jacobsen J, Lee MH, Nagase H, Wewer UM, Murphy G. Selective inhibition of ADAM12 catalytic activity through engineering of tissue inhibitor of metalloproteinase 2 (TIMP-2). Biochem J. 2010; 430:79–86. [PubMed: 20533908]
32. Hougaard S, Loechel F, Xu X, Tajima R, Albrechtsen R, Wewer UM. Trafficking of human ADAM 12-L: retention in the trans-Golgi network. Biochem Biophys Res Commun. 2000; 275:261–7. [PubMed: 10964655]
33. Cardiff RD, Anver MR, Gusterson BA, Hennighausen L, Jensen RA, Wakefield LM, et al. The mammary pathology of genetically engineered mice: the consensus report and recommendations from the Annapolis meeting. Oncogene. 2000; 19:968–88. [PubMed: 10713680]
34. Lin EY, Jones JG, Li P, Zhu L, Whitney KD, Muller WJ, et al. Progression to malignancy in the polyoma middle T oncoprotein mouse breast cancer model provides a reliable model for human diseases. Am J Pathol. 2003; 163:2113–26. [PubMed: 14578209]
35. Livak KJ, Schmittgen TD. Analysis of relative gene expression data using real-time quantitative PCR and the 2(-Delta Delta C(T)) Method. Methods. 2001; 25:402–8. [PubMed: 11846609]
36. Sundberg C, Thodeti CK, Kveiborg M, Larsson C, Parker P, Albrechtsen R, et al. Regulation of ADAM12 cell-surface expression by protein kinase C epsilon. J Biol Chem. 2004; 279:51601–11. [PubMed: 15364951]
37. Dyczynska E, Sun D, Yi H, Sehara-Fujisawa A, Blobel CP, Zolkiewska A. Proteolytic processing of delta-like 1 by ADAM proteases. J Biol Chem. 2007; 282:436–44. [PubMed: 17107962]
38. Carl-McGrath S, Lendeckel U, Ebert M, Roessner A, Rocken C. The disintegrin-metalloproteinases ADAM9, ADAM12, and ADAM15 are upregulated in gastric cancer. Int J Oncol. 2005; 26:17–24. [PubMed: 15586220]
39. Roy R, Moses MA. ADAM12 induces estrogen-independence in breast cancer cells. Breast Cancer Res Treat. 2011
40. Fleming JM, Miller TC, Meyer MJ, Ginsburg E, Vonderhaar BK. Local regulation of human breast xenograft models. J Cell Physiol. 2010; 224:795–806. [PubMed: 20578247]
41. Asakura M, Kitakaze M, Takashima S, Liao Y, Ishikura F, Yoshinaka T, et al. Cardiac hypertrophy is inhibited by antagonism of ADAM12 processing of HB-EGF: metalloproteinase inhibitors as a new therapy. Nat Med. 2002; 8:35–40. [PubMed: 11786904]
42. Horiuchi K, Le GS, Schulte M, Yamaguchi T, Reiss K, Murphy G, et al. Substrate selectivity of epidermal growth factor-receptor ligand sheddases and their regulation by phorbol esters and calcium influx. Mol Biol Cell. 2007; 18:176–88. [PubMed: 17079736]
43. Yarden Y, Sliwkowski MX. Untangling the ErbB signalling network. Nat Rev Mol Cell Biol. 2001; 2:127–37. [PubMed: 11252954]
44. Blobel CP. ADAMs: key components in EGFR signalling and development. Nat Rev Mol Cell Biol. 2005; 6:32–43. [PubMed: 15688065]
45. Blobel CP, Carpenter G, Freeman M. The role of protease activity in ErbB biology. Exp Cell Res. 2009; 315:671–82. [PubMed: 19013149]
46. Atfi A, Dumont E, Colland F, Bonnier D, L'Helgoualc'h A, Prunier C, et al. The disintegrin and metalloproteinase ADAM12 contributes to TGF-beta signaling through interaction with the type II receptor. J Cell Biol. 2007; 178:201–8. [PubMed: 17620406]
47. Iba K, Albrechtsen R, Gilpin B, Frohlich C, Loechel F, Zolkiewska A, et al. The cysteine-rich domain of human ADAM 12 supports cell adhesion through syndecans and triggers signaling events that lead to beta1 integrin-dependent cell spreading. J Cell Biol. 2000; 149:1143–56. [PubMed: 10831617]
48. Thodeti CK, Albrechtsen R, Grauslund M, Asmar M, Larsson C, Takada Y, et al. ADAM12/syndecan-4 signaling promotes beta 1 integrin-dependent cell spreading through protein kinase Calpha and RhoA. J Biol Chem. 2003; 278:9576–84. [PubMed: 12509413]
49. Thodeti CK, Frohlich C, Nielsen CK, Takada Y, Fassler R, Albrechtsen R, et al. ADAM12-mediated focal adhesion formation is differently regulated by beta1 and beta3 integrins. FEBS Lett. 2005; 579:5589–95. [PubMed: 16213489]
50. Thodeti CK, Frohlich C, Nielsen CK, Holck P, Sundberg C, Kveiborg M, et al. Hierarchy of ADAM12 binding to integrins in tumor cells. Exp Cell Res. 2005; 309:438–50. [PubMed: 16061220]

51. Lafuste P, Sonnet C, Chazaud B, Dreyfus PA, Gherardi RK, Wewer UM, et al. ADAM12 and alpha9beta1 integrin are instrumental in human myogenic cell differentiation. Mol Biol Cell. 2005; 16:861–70. [PubMed: 15574885]
52. Eto K, Puzon-McLaughlin W, Sheppard D, Sehara-Fujisawa A, Zhang XP, Takada Y. RGD-independent binding of integrin alpha9beta1 to the ADAM-12 and -15 disintegrin domains mediates cell-cell interaction. J Biol Chem. 2000; 275:34922–30. [PubMed: 10944520]
53. Zhao Z, Gruszczynska-Biegala J, Cheuvront T, Yi H, von der MH, von der MK, et al. Interaction of the disintegrin and cysteine-rich domains of ADAM12 with integrin alpha7beta1. Exp Cell Res. 2004; 298:28–37. [PubMed: 15242759]
54. Huang J, Bridges LC, White JM. Selective modulation of integrin-mediated cell migration by distinct ADAM family members. Mol Biol Cell. 2005; 16:4982–91. [PubMed: 16079176]
55. Cordes N, Seidler J, Durzok R, Geinitz H, Brakebusch C. beta1-integrin-mediated signaling essentially contributes to cell survival after radiation-induced genotoxic injury. Oncogene. 2006; 25:1378–90. [PubMed: 16247454]
56. Giguere Y, Charland M, Bujold E, Bernard N, Grenier S, Rousseau F, et al. Combining biochemical and ultrasonographic markers in predicting preeclampsia: a systematic review. Clin Chem. 2010; 56:361–75. [PubMed: 20044446]
57. White DE, Kurpios NA, Zuo D, Hassell JA, Blaess S, Mueller U, et al. Targeted disruption of beta1-integrin in a transgenic mouse model of human breast cancer reveals an essential role in mammary tumor induction. Cancer Cell. 2004; 6:159–70. [PubMed: 15324699]
58. Chabottaux V, Noel A. Breast cancer progression: insights into multifaceted matrix metalloproteinases. Clin Exp Metastasis. 2007; 24:647–56. [PubMed: 17968664]
59. Massague J. TGFbeta in Cancer. Cell. 2008; 134:215–30. [PubMed: 18662538]
60. Anderberg C, Li H, Fredriksson L, Andrae J, Betsholtz C, Li X, et al. Paracrine signaling by platelet-derived growth factor-CC promotes tumor growth by recruitment of cancer-associated fibroblasts. Cancer Res. 2009; 69:369–78. [PubMed: 19118022]
61. Solomon E, Li H, Muggy SD, Syta E, Zolkiewska A. The role of SnoN in transforming growth factor beta1-induced expression of metalloprotease-disintegrin ADAM12. J Biol Chem. 2010; 285:21969–77. [PubMed: 20457602]
62. Kim BG, An HJ, Kang S, Choi YP, Gao MQ, Park H, et al. Laminin-332-rich tumor microenvironment for tumor invasion in the interface zone of breast cancer. Am J Pathol. 2011; 178:373–81. [PubMed: 21224074]

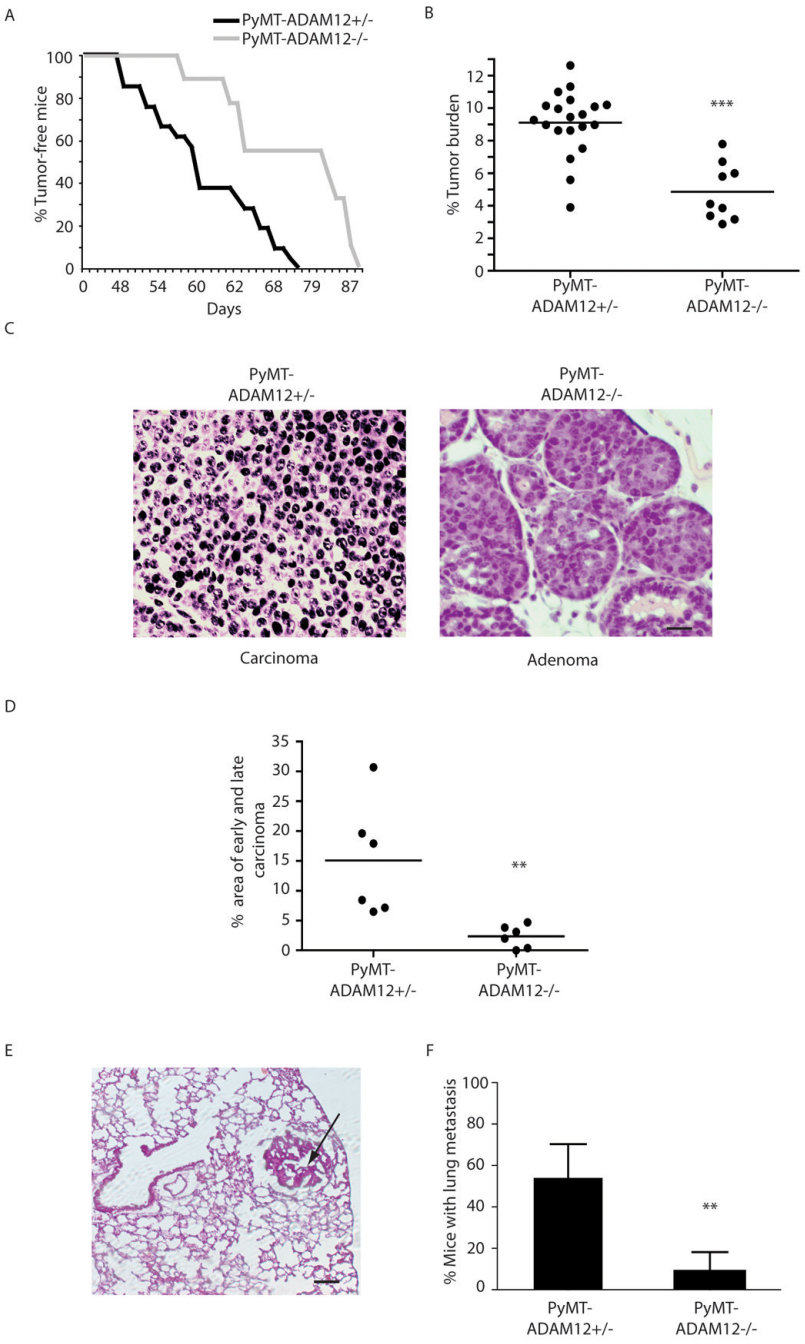

Figure 1. ADAM12 deficiency suppresses mammary tumorigenesis

A, Kaplan-Meier analysis of tumor onset in PyMT-ADAM12+/- (n=21) and PyMT-ADAM12-/-mice (n=11). *B*, Mean (±SD) tumor burden (total tumor mass/mouse weight in percentage) in PyMT-ADAM12+/- (n=21) and PyMT-ADAM12-/- (n=11) mice at 12 weeks of age. *C*, Representative H&E-stained histological sections of carcinomas and areas of adenoma in tumors from PyMT-ADAM12+/- and PyMT-ADAM12-/- mice. Bar = 30 μm. *D*, Mean (±SD) area of early and late carcinoma in the mammary-gland tumors of PyMT-ADAM12+/- (n=6) and PyMT-ADAM12-/- (n=6) mice. *E*. Representative figure of a metastasis (arrow) in the peripheral part of the lung, bar = 100 μm. *F*. Percentage of animal bearing at least one tumor nodule in PyMT-ADAM12+/- (n=11) and PyMT-ADAM12-/-

(n=11) mice. Log rank were used in *A*, Student t test in *B* and *D*, and Wilcoxon signed-rank test in *F*. ** $P < 0.01$, *** $P < 0.001$

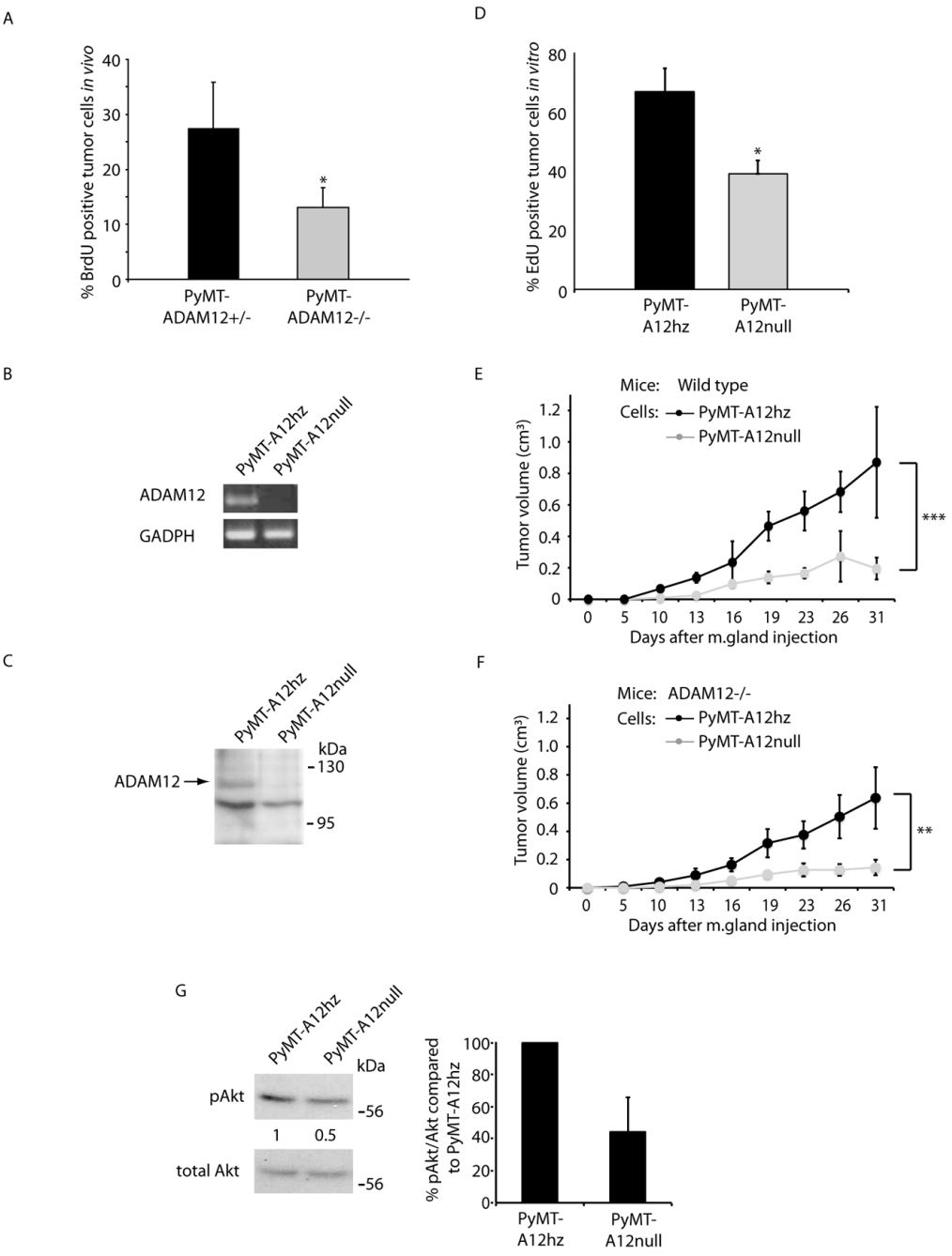

Figure 2. ADAM12 affects tumor cell proliferation of PyMT cells *in vivo* and *in vitro*

A, Mean (±SD) cell proliferation assessed by BrdU incorporation in PyMT-ADAM12+/- (n=5; total cells: 18435) and PyMT-ADAM12-/- (n=5; total cells: 12949) tumors. *B-C*, Expression of ADAM12 total RNA (*B*) and protein (*C*) in immortalized PyMT-A12hz and PyMT-A12null tumor cells examined by RT-PCR and Western blot, respectively. GAPDH served as a reference gene. *D*, Mean (±SD) cell proliferation assessed by EdU incorporation in immortalized PyMT-A12hz (n=386) and PyMT-A12null (n=427) tumor cells. The data are representative of 3 independent experiments. *E*, Mean (±SD) tumor volumes over time in wild-type mice on FVB/N genetic background injected with PyM-A12hz (n=9) or PyMT-A12null (n=9) immortalized tumor cells in the mammary gland (m.gland). *F*, Mean (±SD)

tumor volumes over time in ADAM12-/- mice on FVB/N genetic background injected with PyM-A12hz (n=5) or PyMT-A12null (n=5) immortalized tumor cells in the m.gland. *G*. Western blot analysis of pAkt and total Akt in PyMT-A12hz and PyMT-A12null tumor cells. The number beneath the pAkt blot and the bar graph depicts Akt activity, which was determined by quantification of the band intensities (using ImageJ image analysis software), calculated as the level of pAkt to total Akt and compared to PyMT-A12hz. The average of 3 independent experiments is shown. **P* < 0.05, ** *P* < 0.01, *** *P* < 0.001.

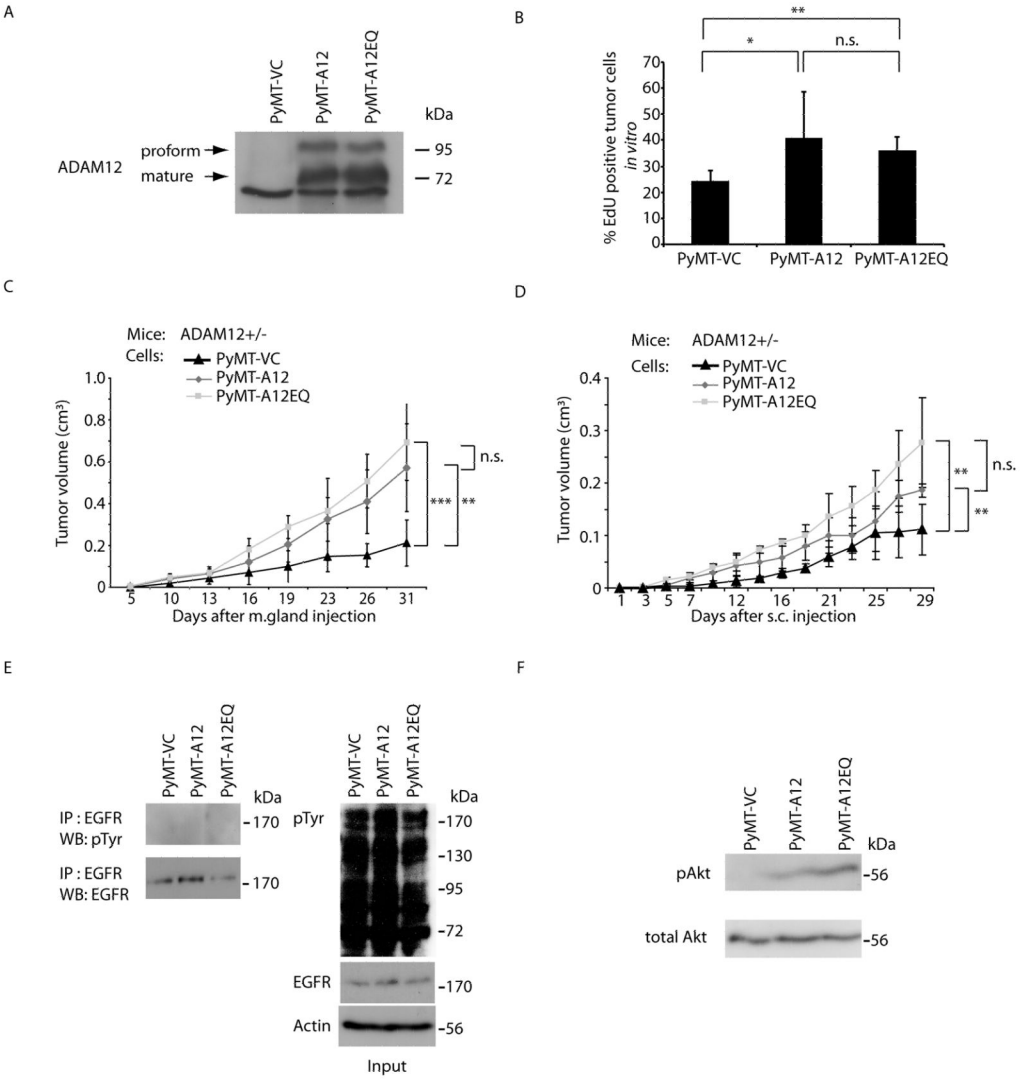

Figure 3. The proteolytic capacity of ADAM12 is dispensable for tumor growth

PyMT-A12null cells stably expressing vector control (PyMT-VC), human ADAM12 lacking the cytoplasmic tail (PyMT-A12), or human ADAM12 lacking the cytoplasmic tail and with a catalytic site mutation (PyMT-A12EQ) were examined. *C*, Western blot analysis of ADAM12 expression in the three cell lines. *D*. Mean (±SD) cell proliferation assessed by EdU incorporation in immortalized PyMT-VC (n=2936), PyMT-A12 (n=948) and PyMT-A12EQ (n=1811) tumor cells. *E*, Mean (±SD) tumor volumes over time in ADAM12+/- mice on FVB/N genetic background injected with PyMT-A12 (n=8), PyMT-A12EQ (n=5), or PyMT-VC (n=7) cells into the mammary-gland (m.gland). *F*, Mean (±SD) tumor volumes over time in ADAM12+/- mice on FVB/N genetic background injected subcutaneously (s.c) with PyMT-A12 (n=5), PyMT-A12EQ (n=4), or PyM-VC (n=5) cells. *E*. (*Left*) EGFR was immunoprecipitated (IP) from PyMT-VC, PyMT-A12, PyMT-A12EQ total tumor cell lysate and were blotted with phosphotyrosine (pTyr). (*Right*) Western blot analysis of pTyr, total EGFR, and Actin from input of PyMT-VC, PyMT-A12, and PyMT-A12EQ tumor cell lysate used for IP (representative from 3 experiment). *F*. Western blot analysis of pAkt and total Akt in PyMT-A12hz and PyMT-A12null tumor cells. The data are representative of 3 independent experiments. n.s. = nonsignificant, *$P < 0.05$, ** $P < 0.01$, *** $P < 0.001$, (*C,D;* based on final volumes).

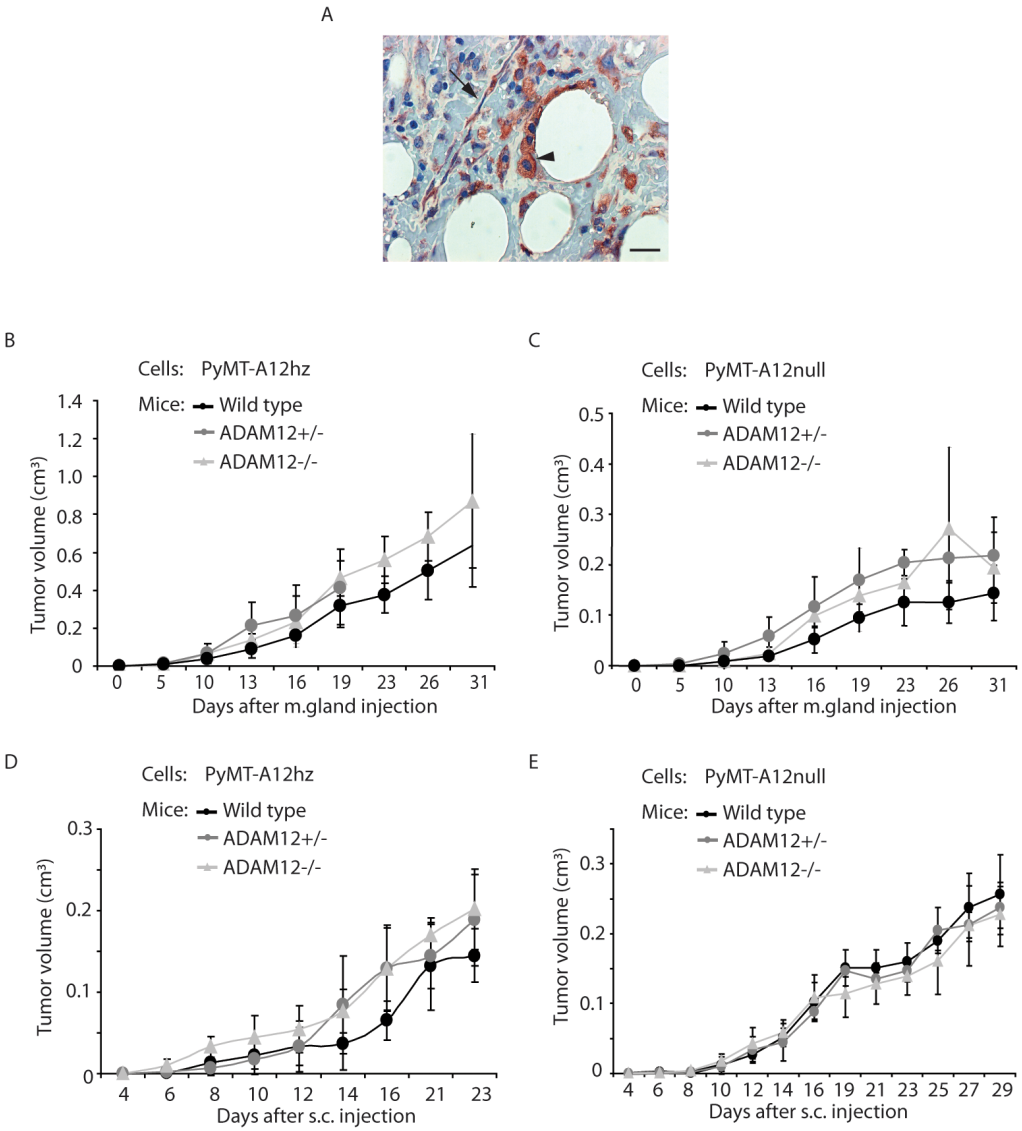

Figure 4. Stromal ADAM12 does not influence tumor growth

A, Immunohistochemical staining of ADAM12 in normal mouse breast tissue using polyclonal antibody against ADAM12 (rb109). Vessels (arrow), and brown fat cells (arrowhead) were positive for ADAM12 immunostaining. Sections were counterstained with hematoxylin, bar = 20um. *B-C*, Mean (±SD) tumor volumes over time in wild-type (n=9), ADAM12+/- (n=7), or ADAM12-/-(n=5) mice on the FVB/N genetic background injected in the mammary gland (m.gland) with PyMT-A12hz *(B)* or PyMT-A12null *(C)* cells. *D-E*, Mean (±SD) tumor volumes over time in wild-type (n=5), ADAM12+/- (n=5), or ADAM12-/- (n=5) mice on the FVB/N genetic background injected subcutaneously (s.c.) in the right flank with PyMT-A12hz *(D)* or PyMT-A12null (*E*) cells.

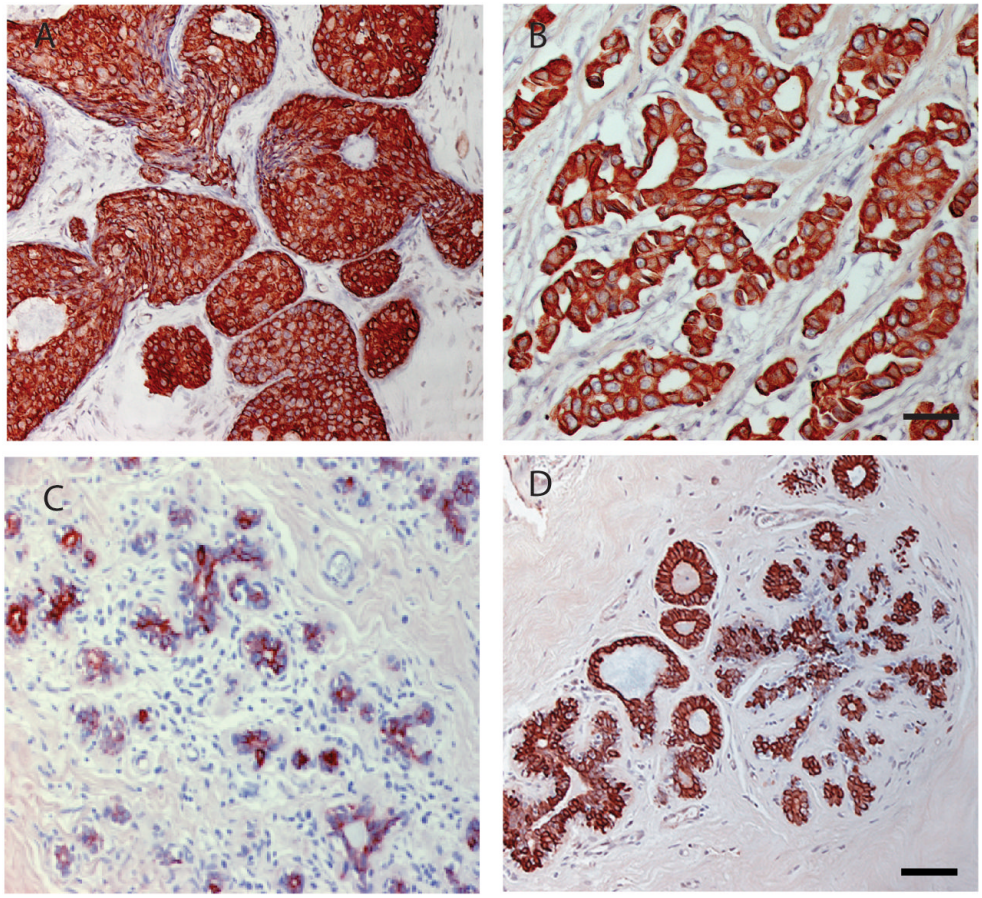

Figure 5. ADAM12 immunolocalization in human benign and malignant breast tissue

Immunohistochemical staining of ADAM12 in DCIS *(A)* IDC (*B*), TDLUs in normal breast tissue from breast-reduction surgery (*C*), and TDLUs adjacent to carcinoma cells *(D)* using an ADAM12 polyclonal antiserum (rb122). Sections were counterstained with hematoxylin. Scale bar in *B* = 40 μm and *D* = 50 μm. A and B use identical magnification, as do C and D.

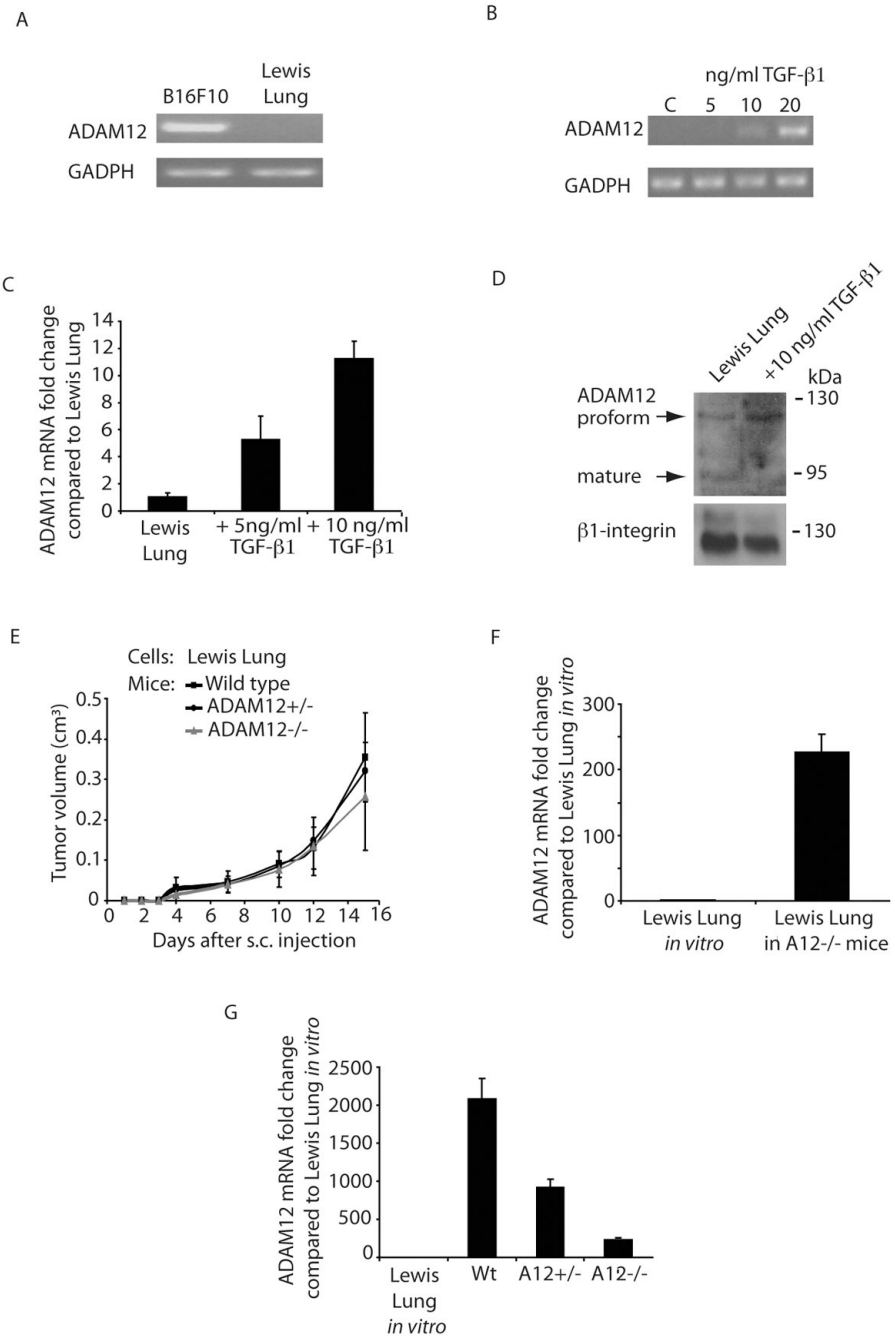

Figure 6. Tumor-associated stroma influences ADAM12 expression

A, ADAM12 expression in B16F10 melanoma and Lewis Lung cells analyzed by RT-PCR. *B*, ADAM12 expression in unstimulated (C) or TGFβ-1-stimulated Lewis Lung cells grown *in vitro* analyzed by RT-PCR. *C*, Relative fold-change of ADAM12 expression in TGF-β1 -stimulated Lewis Lung cells grown *in vitro* compared with unstimulated Lewis Lung cells examined by qPCR. Error bars represent standard deviation calculated from triplicate qPCR reactions. D, Western blot analysis of ADAM12 expression in unstimulated or TGFβ-1-stimulated Lewis Lung cells grown *in vitro*. β1-integrin serves as loading control. *E*, Mean (±SD) tumor volumes over time in wild-type (n=4), ADAM12+/- (n=8), or ADAM12-/- (n=8) mice on the C57/Bl6 genetic background injected subcutaneously (s.c.) in the right

flank with Lewis Lung cells. *F*, Mean (±SD) relative fold-change of ADAM12 expression in Lewis Lung cells grown *in vitro* and Lewis Lung tumors grown in ADAM12-/- mice (n=8) analyzed by qPCR. *G*, Mean (±SD) relative fold-change of ADAM12 expression in Lewis Lung cells grown *in vitro* and Lewis Lung tumors grown in wild-type (n=4), ADAM12+/- (n=8), or ADAM12-/- (n=8) mice (as described in *E*) analyzed by qPCR. For *A* and *B*, GAPDH served as a reference gene. For *C*, *F*, and *G*, rPO was used as a reference gene, Lewis Lung *in vitro* was set to a value of 1, and the results were verified in at least three independent biological experiments.

Table 1

Table 1A. ADAM12 immunostaining of six different breast cancer tissue arrays

Arrays	Cases	Positive	%	Diagnosis	Origin
YTMA 12	338	227	67.2	322 IDC, 12 ILC, 4 others	Yale Uni, USA
YTMA 10A	325	167	51.4	271 IDC, 45 ILC, 9 others	Yale Uni, USA
Zymed 57-7043	51	42	82.4	51 IDC	Zymed, Ca, USA
Zymed ID10011	47	34	72.3	44 IDC, 3 ILC	Zymed, Ca, USA
PAK1	22	17	77.3	18 IDC, 4 ILC	Turku Uni, Finland
PAK2	22	18	81.8	20 IDC, 2 ILC	Turku Uni, Finland
Total	805	505	62.7	726 IDC, 66 ILC, 13 others	

Table 1B. ADAM12 immunohistochemical evaluation (distribution, staining intensity (0, no staining; 1, weakly; 2, moderate; 3, strongly stained) membrane, cytoplasmic localization) on whole mount breast material from 61 cases

Diagnosis	n =	Positivity (%)	Intensity (0-3) (± st. error)	Membr (%)	Cytopl (%)	Membr + Cytopl (%)
ADH	9	77	2.6 (±0.2)	0	56	44
DCIS	7	84	2.5 (±0.2)	0	57	43
IDC	33	47	1.8 (±0.1)	42	19	39
ILC	9	97	3.0 (±0.0)	0	92	8
Other	3	96	2.3 (±0.3)	33	33	34

Table 1C. ADAM12 immunohistochemical evaluation (distribution, staining intensity (0, no staining; 1, weakly; 2, moderate; 3, strongly stained) membrane, cytoplasmic localization) of TDLUs in whole mount material in 10 non-tumorous cases and in 45 cases of invasive carcinomas

Diagnosis	Positivity (cells) (%)	Intensity (0-3) (± st. error)	Membr (%)	Cytopl (%)	Membr + Cytopl (%)
Non-tumorous TDLU	28	1.6 (±0.22)	60	0	40
Invasive carcinomas TDLU	89	2.9 (±0.06)	0	81	19

Atypical ductal hyperplasia (ADH), ductal carcinoma in situ (DCIS), infiltrating ductal carcinomas (IDC), infiltrating lobular carcinomas (ILC), terminal ductal lobular units (TDLU)